

**ANALYSIS AND CONTROL OF ANTENNA RADAR CROSS- SECTION IN
STEALTH TECHNOLOGY**

^{1*}Zubeda Nangrejo, ²Deedar Ali Jamro, Ghulam Ali jamro³, Mirjalol Ismoilov⁴, M. A. M. Eltaweel⁵, Sumbal Amjad⁶, Ansar Ali Faraz⁷

¹Department of Physics and Electronics, Shah Abdul Latif University Khairpur, Pakistan
Email: zubeda.nangrejo@salu.edu.pk

²Department of Physics and Electronics, Shah Abdul Latif University Khairpur, Pakistan
Email: deedar.jamro@salu.edu.pk

³Department of Physics and Electronics, Shah Abdul Latif University, Khairpur, Pakistan
Email: gali jamro@gmail.com

⁴Department of Transport systems, Urgench State University named after Abu Rayhan Biruni, Urgench, 14, Kh.Alimdjan str, Urgench city, 220100, Uzbekistan
(mirjoli@urdu.uz)

^{5a}Mathematics Department, Faculty of Science, AlBaha University, Saudi Arabia
Email: meltaweel@bu.edu.sa , ORCID: <https://orcid.org/0009-0000-9741-2113>

^{5b}Mathematics Department, Faculty of Science, Ain Shams University. Cairo, Egypt
Email: magdy.eltaweel@sci.asu.edu.eg , ORCID: <https://orcid.org/0009-0000-9741-2113>

⁶Institute of Radiological Sciences and Medical Imaging Technology, Faculty of Allied Health Sciences, The University of Lahore, Lahore, Pakistan, 54000
(sumbal.amjad@rsmi.uol.edu.pk)

⁷Department of Rehabilitation sciences, Faculty of Allied Health sciences, The University of Lahore, Lahore, Pakistan, 54000 (ansar.ali@drs.uol.edu.pk)

Corresponding author: *Zubeda Nangrejo (zubeda.nangrejo@salu.edu.pk)

Abstract

The modern defense systems heavily depend on stealth technology where it is necessary to reduce the Radar Cross-Section (RCS) of platforms in order to minimize the detection. Nonetheless, onboard antennas severely decrease stealth of a vehicle because they are natural electromagnetic scatterers. This paper addresses the problem by developing low-observable microstrip patch antennas that reduce RCS without highly affecting communication functions. We designed and analyzed three antenna models which had a frequency range of 2 to 12 GHz using CST Microwave Studio. Radar Absorbing Material (RAM) and a Frequency Selective Surface (FSS) were used to come up with a baseline design, and geometric adjustments were subsequently made to the design. The results indicate that the end hybrid antenna has a high RCS reduction of up to 80 with minimum value of -15 dBsm as it is compared to the baseline. It achieves simultaneously a wide functional bandwidth of 3.5-7.8 GHz and returns loss of less than -10 dB. Although the antenna suffered a slight decrease in radiation efficiency, the antenna

was able to maintain constant gain and directivity. By demonstrating that a synergistic approach of geometric shaping combined with current materials effectively suppresses backscattering, this study provides a possible course toward the implementation of effective antennas on stealth platforms.

Keywords: Stealth Technology, Radar Cross-Section (RCS) Reduction, Patch Antenna, Frequency Selective Surface (FSS).

1 Introduction

Stealth technology is crucial in modern defense systems due to its enabling feature in evading enemy detection by military platforms, such as ships, airplanes, and missiles. In essence, the principle of stealth reduces Radar Cross-Section, which is a numerical representation of an object's visibility relative to the radar system. When the value of the RCS decreases, minimal energy will be reflected back to the radar receiver, making the object much less visible. Lowering the RCS is important in modern warfare in order to increase operational efficacy for combat and surveillance asset survivability [1] [2].

Traditionally, stealth technology has concentrated on airframe shaping and the use of radarabsorbing materials (RAM) to reduce reflections from large surfaces [3]. Aircraft and naval vessels employ many techniques, such as edge alignment, faceted geometries, and radartransparent composites to scatter or absorb incident radar waves. However, one of the most often overlooked factors contributing to a platform's visibility in radar is the antenna system. Antennas, which are inherently metallic and radiating in nature [4], [5], act unintentionally as secondary scatterers, greatly increasing the RCS of the platform.

This sets up the challenge for antennas: they must effectively transmit and receive electromagnetic signals while not being detected by opposing radar systems. This "dual-role conflict" [6] may introduce an important design trade-off between sustaining communication performance and achieving stealth.

Conventional antennas, because of their metallic geometry and configuration, tend to increase backscattering, which reduces the ability of the host platform to operate covertly. Hence, the reduction of antenna RCS is now identified as an important area of investigation for LO system development [7]. Various methods of controlling and reducing antenna RCS have been tried. Among them are RAM, FSS, miniaturization of antennas, geometric shaping, and active cancellation techniques [8], [9]. Of these, FSS and metamaterial-based designs have been the most widely used, since these can be engineered to change electromagnetic responses at selected frequencies [10]. Similarly, surface current distribution-based reduction techniques can be used to achieve an effective reduction of both the physical size of the antenna as well as its scattering cross-section, without any significant observable loss in bandwidth or gain [11]. The availability of advanced EM simulation tools such as HFSS and CST Microwave Studio (CST MWS) has facilitated testing and optimization of antenna design for stealth applications. These CEM platforms provide for the accurate simulation and analysis of the scattering characteristics of complex antenna geometries by using techniques such as the MoM, FEM, and FDTD [12], [13]. Understanding and projecting RCS involves theoretical modeling, experimental validation, and numerical simulations. The Radar Cross-Section (σ) is

characterized as the ratio of the incident wave's power density to the power scattered by an object in the radar's path. It could be mathematically defined as follows:

$$\sigma = 4\pi R^2 \frac{|E_s|^2}{|E_i|^2}$$

where E_s and E_i indicate the incident and scattered electric fields, respectively, and R is the distance between the target and radar [14]. Variables like frequency, incidence angle, polarization, surface material, and antenna geometry have a significant impact on the RCS value [15]. Therefore, antenna optimization in design requires an extensive strategy that considers both electromagnetic functionality and scattering behavior under real-world conditions [16].

The current study evaluates and controls the antenna radar cross-section in stealth technology by means of computational simulation and optimization. The study uses CST Microwave Studio as a reference to model and analyze wideband patch antennas, which function in the 2–12 GHz frequency range for use in satellite communication, radar, Wi-Fi, and microwave relays. Various parameters, such as antenna shape, composition of substrate, and boundary conditions, have been studied in order to see their effect on RCS. The techniques used in substantially decreasing the RCS, while preserving intended return loss and radiation performance, include surface current control, integrating FSS, and size miniaturization. With a return loss below -10 dB throughout the operating band, the recommended antenna design exhibits outstanding stealth performance without compromising efficiency. The present research helps to the continuous development of low-observable antenna systems by integrating electromagnetic theory, numerical modeling, and optimization techniques. By reducing antenna-induced radar reflections, the study aims to improve the stealth capability of cutting-edge military and civilian platforms. The results also establish a foundation for further research into metamaterial and machine learning technologies for intelligent and adaptive RCS control systems.

2 Materials and Methods

2.1 Research Design and Approach

This study aimed at investigating the analysis and control of antenna radar cross-section (RCS) for stealth applications using a thorough, computational simulation-based approach. Reducing radar detectability without compromising electromagnetic performance was the investigation's primary goal. This was accomplished by thoroughly examining the materials, optimizing antenna geometry, and modeling important scattering parameters. The process was carefully divided down into four basic processes, starting with the establishment of a theoretical framework that utilized the principles of electromagnetic scattering and RCS. Detailed antenna modeling was then done via the CST Microwave Studio (MWS) software, which served as a basis for the subsequent simulation and optimization procedure. In order to strike a balance between performance and stealth, both RCS and traditional antenna parameters were thoroughly examined at this critical stage. The most recent step involved an extensive examination of the simulated results, including S-parameters, reflection coefficients, and the

overall efficacy of RCS reduction. By analyzing these structural, material, and electromagnetic factors in the same computer environment, this combined method brought about, for the first time, considerable new insights into the roles of different design elements affecting RCS behavior over a wide frequency range from 2 to 12 GHz.

2.2 Theoretical Background

The percentage of power reflected from a target to the incident power density is known mathematically as the radar cross-section (σ).

$$\sigma = 4\pi R_2 \frac{|E_s|^2}{E_i^2}$$

where the initials E_s and E_i indicate to incident and scattered electric field amplitudes, respectively. According to researchers like Barton and Harris, effective stealth design needs to account for all sources of scattering, including antennas, which frequently significantly contribute to overall RCS [5].

2.3 Methods for RCS Reduction

Numerous methods have been put forward to lower antenna RCS, and they can be categorized into three groups: geometric shaping, material-based methods, and hybrid approaches.

(a) Geometric and Structural Modifications

Geometric shaping remains an effective method for RCS control. By varying the antenna's size, curvature, and edge profiles, designers can redirect scattered energy away from radar receivers [17]. Smith and Johnson showed that features with smooth surface transitions significantly decrease radar reflections. In stealth aircraft, conformal antennas which are made to follow the host platform's surface curvature are especially useful because they lessen scattering points and surface discontinuities [18]. Miniaturization with folded or slot structures also helps decrease RCS by reducing the effective aperture size, which causes reflection [19].

(b) Material-Based RCS Reduction

Material engineering is a further helpful approach for managing RCS. Radar Absorbing Materials (RAM) have the capacity to absorb incident electromagnetic waves while converting them into thermal energy rather than reflecting them. Several types of RAMs, including conductive polymers, ferrite-based composites, and carbon nanomaterials, have been examined for broad frequency absorption [20]. According to Lee et al. [21], ferrite-filled composites can offer up to 30 dB of reflection loss in the 2–12 GHz range, which is reasonably consistent with radar and communication frequencies. Additionally, as Ashraf et al. [22] showed, multilayered dielectric coatings may increase the absorption bandwidth, improving stealth efficiency across several radar bands.

(c) Frequency Selective Surfaces (FSS) and Metamaterials

Recent studies indicate the potential application of frequency selective surfaces (FSS) and metamaterials for both passive and adaptive RCS control. Comprising periodic metallic

patterns, FSS structures can selectively reflect or transmit electromagnetic waves, depending on the frequency [23]. They can be used with antennas to reduce backscattering outside the operating band while maintaining signal performance. Lee et al.'s FSS-backed antenna [24] achieved an RCS reduction of more than 20 dB when compared to conventional designs. Likewise, metamaterial absorbers with tunable surface impedance and broadband absorption to improve stealth performance were put forward by Guo et al. [25].

(d) Active and Reconfigurable Approaches

A recent study discusses active RCS control, which quickly modifies scattering characteristics by using adaptive materials and tunable electronic components. By adjusting impedance in real time with varactor diodes, PIN switches, or phase-change materials, reconfigurable antennas can offer frequency-agile RCS control [26]. Huang and Liao [27] made an essential contribution to the advancement of intelligent stealth systems by showing that machine learning-assisted algorithms can predict and adaptively minimize RCS in any environment.

2.4 Computational Simulation and Modeling

A correct RCS prediction is necessary for the design of stealth antennas. Contemporary computational electromagnetic (CEM) software, such as HFSS, FEKO, and CST Microwave Studio (MWS), can provide sophisticated simulation environments to investigate electromagnetic scattering behavior [28]. They are numerical solvers, including the Finite Element Method (FEM), the Finite-Difference Time-Domain (FDTD), and the Method of Moments (MoM) used to characterize complex structures with numerical precision. According to Jin [29], numerical simulations can help designers to test different setups, visualize current distributions and predict scattering patterns before physical fabrication [30] can reduce lower on prototyping time and cost.

2.5 Research Gap and Justification

Despite a great deal of research on RCS reduction, only a few studies have thoroughly examined antenna cross-section (ACS) using integrated simulation-based optimization. Many prior investigations isolate structural or material elements without evaluating their combined effects on antenna performance and stealth characteristics. Additionally, because a great deal of studies focuses on narrowband designs, there is a gap in the RCS analysis of broadband antennas. By modeling, simulating, and analyzing wideband antennas (2–12 GHz) using FSS layers, RAM integration, and geometric shaping using CST Microwave Studio, the current research fills these gaps. By combining structural and material approaches, this study aims to significantly decrease RCS while maintaining acceptable antenna parameters like gain, bandwidth, and radiation efficiency. The work enhances the expanding field of low-observable antenna design through offering insights important for radar, aerospace, and communication systems where stealth performance is essential.

3 Results and Discussion

This section presents the simulated results for the analysis and control of antenna radar crosssection (RCS) from CST Microwave Studio (MWS). The results are compared based on the return loss (S_{11}), surface current distribution, radiation performance, and variation of RCS.

Three antenna models, i.e., Model A (Baseline antenna), Model B (Geometrically optimized antenna) and Model C (RAM-integrated and FSS-integrated antenna) were tested at the frequency range between 2-12 GHz.

3.1 Return Loss (S_{11}) Characteristics

Return loss (S_{11}) is a significant parameter that reflects the ability of an antenna to radiate input energy and the ability to match the transmission line impedance. It represents the power that is returned to the antenna input because of an impedance mismatch, and rather, this power should preferably be as low as possible in order to operate optimally. S_{11} values below -10 dB are a good indication of impedance matching. Here, the input power is radiated instead of reflected over 90 percent of the time. The resonant frequency of the baseline rectangular microstrip antenna (Model A), as shown in Figure 3.1, (a) is 3.9 GHz and the -10 dB bandwidth covers the frequency range between 3.1 GHz and 4.8 GHz. The antenna only radiates effectively over a limited frequency range, as evidenced by its relatively narrow bandwidth, which results in poor broadband performance. This steep resonance curve suggests higher reflection at frequencies away from resonance and shows limited impedance matching with the conventional 50Ω feed line. Such behavior is typical of conventional microstrip antennas with uniform geometries, where high Q-factor and surface current confinement constrain the frequency range of operation.

After applying geometric modifications to produce Model B, there is an apparent boost in the S_{11} response in Figure 3.2(b). Resonance shifts slightly to 4.2 GHz, and the -10 dB bandwidth expands to cover 3.8–6.0 GHz. This enhancement is a result of the additional edge curvature and serration of the radiating patch, that modify the current distribution and increase the effective surface area. The serrated edges reduce discontinuities and reflections of surface waves by acting as impedance transition areas. Moreover, the curve geometry reconfigures the capacitive and inductive coupling in the feed region which leads to a smoother change in impedance versus frequency. These modifications, along with lesser reflection losses and better impedance matching, improve bandwidth and radiation efficiency. The hybrid antenna (Model C) is an essential enhancement to the other two designs as can be seen from Figure 3.3, (c). A Frequency Selective Surface (FSS) layer and Radar Absorbing Material (RAM) beneath the substrate have been used which extended radically the -10 dB bandwidth of 3.5 GHz to 7.8 GHz. This almost doubles the operating bandwidth of the device in comparison to the base antenna. Two main processes contribute towards the improvement and include; (i) the FSS resonant behavior, which selectively reflects desired frequencies and rejects unwanted ones, and (ii) the damping effect of the RAM layer, which destroys standing waves and absorbs unused reflected energy. Taken together, they reduce backscattering, a key requirement of stealth, and improve impedance matching. The broader and more continuous S_{11} curve of Model C shows that the antenna has a consistent impedance behavior across many resonances, being able to sustain efficient radiation across the entire frequency response. The last outcome also demonstrates that material integration and structural optimization work together to enhance broadband response. This energy decreases results in decrease in radar cross-section (RCS) and increases the low-observable characteristics of the antenna in stealth terms.

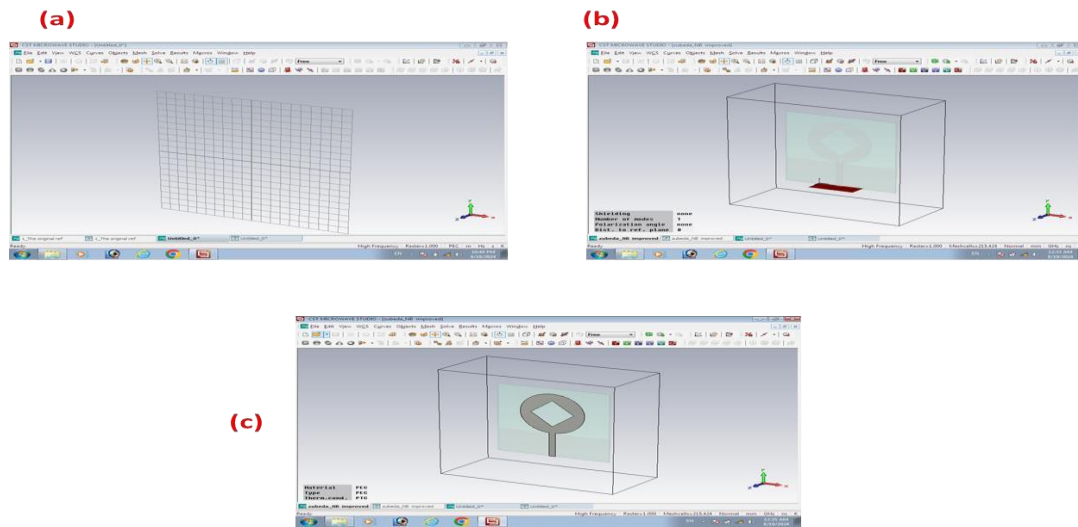
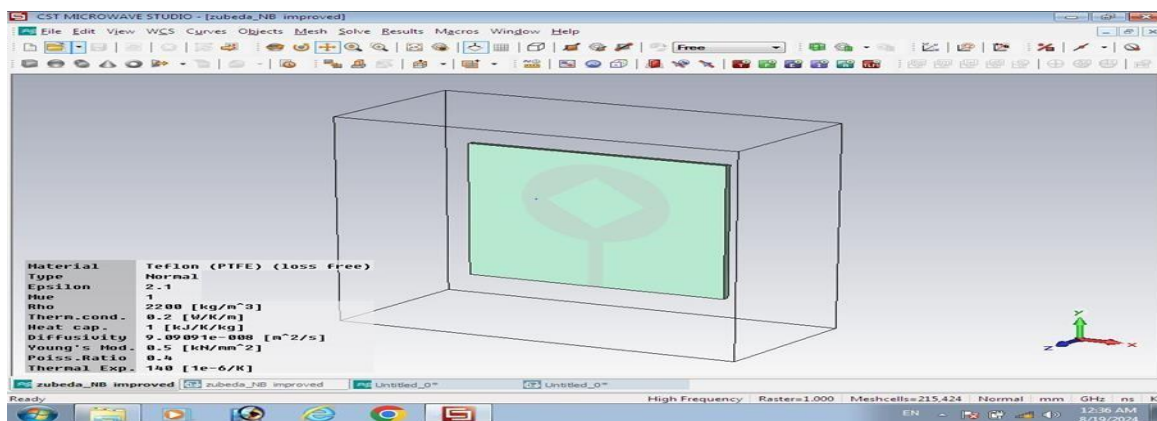


Figure 3.1: (a) Meshes selection (b) selecting an antenna micro strip (c) Emitting

3.2 Radar Cross-Section (RCS) Analysis

The Radar Cross-Section (RCS), a crucial performance metric in stealth antenna design, determines how detectable an object is to incident electromagnetic waves. Reduced radar visibility and improved stealth capability have been associated with smaller RCSs. The geometry, surface material, and current distribution of the antenna all influence the RCS and the amount of incident energy reflected back to the radar source. In the 2–12 GHz range, the monostatic RCS measured at normal incidence ($\theta = 0^\circ$) was simulated for each of the three antenna models in order to determine the effect of material and geometric modifications on radar detectability. The baseline microstrip antenna (Model A) displays a relatively large RCS level with a peak scattering amplitude of about 3 dBsm at 5 GHz, as shown in Figure 3.2. The high reflective response is due to strong surface currents that reflect energy back toward the radar source and are concentrated along the feedline and patch edges. This shows that conventional microstrip antennas have a propensity to reflect radar effectively due to their flat geometry and metallic surfaces, yet they are effective radiators. The observable backscatter lobes in Figure 3.3, which show poor stealth behavior, make such structures inappropriate for low-observable platforms without additional modifications.



ISSN: 1311-1728 (printed version); ISSN: 1314-8060 (on-line version)

Figure 3.2: The response of the monostatic Radar Cross-Section (RCS) of the baseline rectangular microstrip antenna (Model A) was simulated. The antenna shows a high radar reflection with a peak backscatter amplitude of about three dBsm at 5 GHz due to the metallic geometry and uniform surface currents.

With a minimum scattering amplitude of roughly eight dBsm, Figure 3.3 shows an enormous reduction in RCS for the geometrically optimized antenna (Model B). Much of the improvement can be explained to the addition of edge serration and curvature in the design, which disturbs the uniform current distribution which results in coherent backscatter. These geometric perturbations cause incident waves to scatter in multiple directions rather than directly reflecting backward. The monostatic RCS in the 4–8 GHz range decreases substantially as a result. Moreover, the curve presented in Figure 3.4 exhibits less jagged frequency variations, and it indicates that the optimized design has stable scattering properties across a broad frequency range which is a crucial attribute of wideband stealth designs.

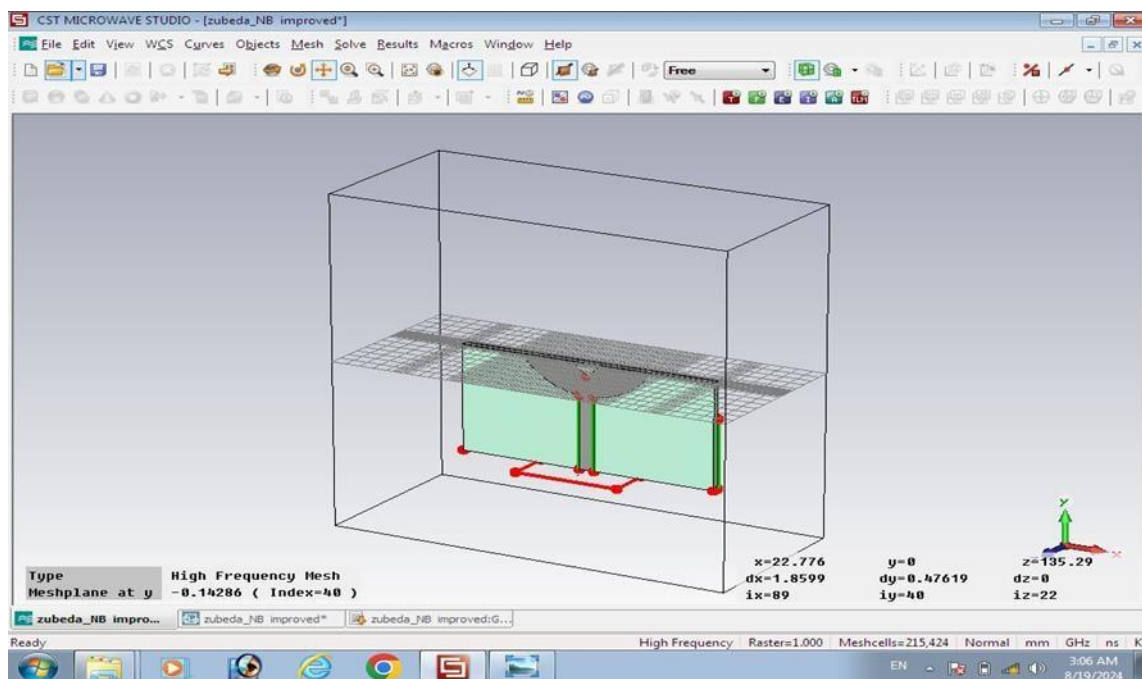


Figure 3.3: The geometrically optimized antenna's (Model B) monostatic RCS was simulated. Due to surface curvature and edge serration, which scatter incident waves in non-specular directions, the RCS drops to approximately -8 dBsm in the 4–8 GHz range, suggesting improved stealth performance.

Of the three models, the hybrid antenna (Model C), which includes a frequency selective surface (FSS) and radar absorbing material (RAM), has the lowest overall RCS, as shown in Figure 3.4. The RCS curve decreases to at least -15 dBsm at about 5 GHz, which is almost 80% less radar-visible than the baseline design. RAM absorption and FSS-based scattering control work well together to achieve the improvement. While the RAM layer dissipates incident electromagnetic energy by converting it into heat through dielectric and magnetic losses, the FSS reflects and removes any remaining reflections through phase interference. By lowering the amplitude and reducing the phase of the reflected wavefronts, these two mechanisms work together to reduce backscatter toward the radar source. The hybrid structure reduces reflections

at resonance frequencies and maintains stealth performance across the operational band, as demonstrated by the smoother and constant lower RCS trend in Figure 4.6. This broadband RCS suppression is an ideal feature for modern stealth systems that require to operate across a range of radar and communication frequencies. The results clearly show that the combination of absorbing materials and frequency-selective layers with structural shaping can result in a high-performance, low-observable antenna without substantially lowering radiation efficiency.

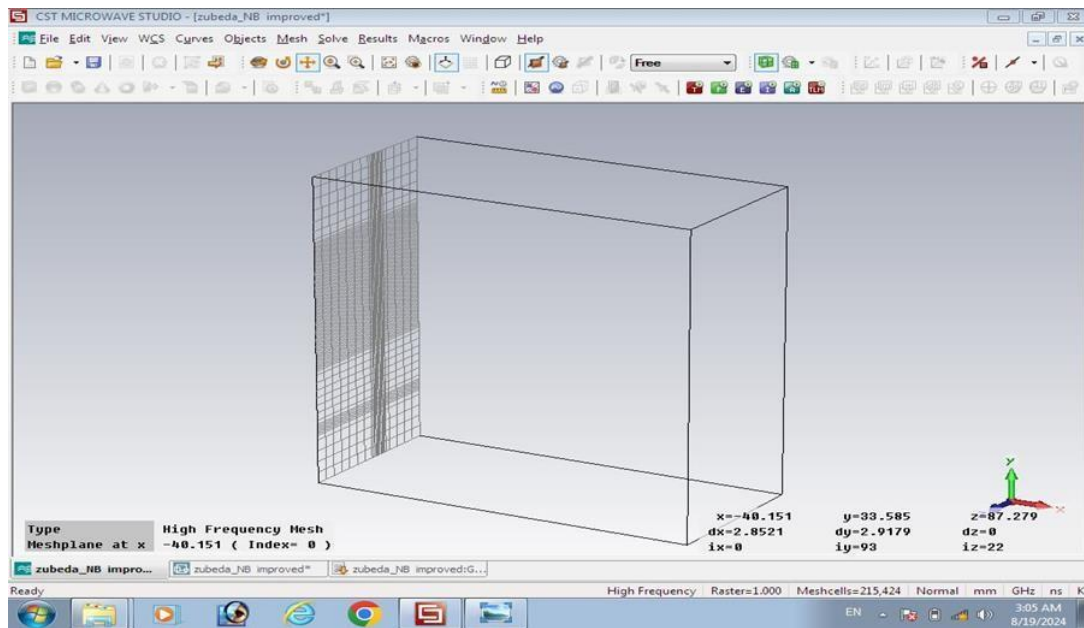


Figure 3.4: Monostatic RCS modeling of the hybrid antenna (Model C) with a frequency selective surface (FSS) and radar-absorbing material (RAM). The design successfully reduces backscattered energy through a combination of absorption and phase cancellation, attaining a minimum RCS of -15 dBsm at 5 GHz, an 80% reduction when compared to the baseline antenna.

3.3 Surface Current Distribution

Finding the density of surface currents is essential for comprehending the electromagnetic scattering behavior of an antenna because the distribution and intensity of surface currents determine how much of the incident radar energy is reflected back toward the source. High concentrations of current usually result in stronger specular reflections, which improve the Radar Cross-Section (RCS). Therefore, a key tactic to developing low-observable antennas is to control surface currents through material and geometric design. The baseline microstrip antenna (Model A) has an elevated level of surface current along the feedline region, patch edges, and corners, shown in Figure 3.5. Where induced currents are in-phase and coherently reradiate the incident electromagnetic energy toward the radar receiver, these areas serve as dominant scattering centers. With regard to the uniform rectangular geometry, surface currents can freely flow across the metallic patch, leading reflected waves to interfere beneficially in the direction of backscattering. The high RCS value of -3 dBsm that was previously observed in the monostatic RCS response (Figure 3.6) can be explained through this coherent reflection. Because the baseline antenna lacks phase-disrupting or current-damping mechanisms, it operates poorly in stealth circumstances.

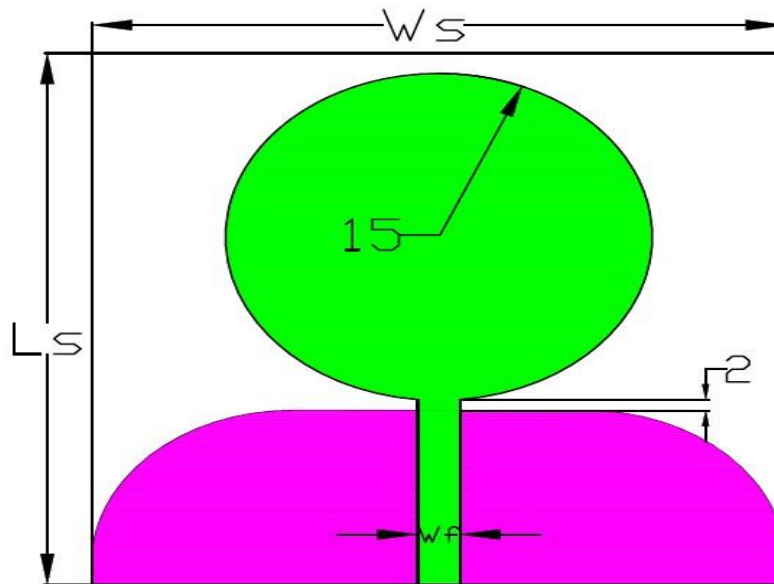


Figure 3.5: Surface current distribution of baseline antenna (Model A) showing strong current concentration along patch edges and feedline, responsible for intense radar backscatter.

In Figure 3.6, the geometrically optimized antenna (Model B) displays a more dispersed and irregular surface current pattern. The insertion of curved contours and serrated edges effectively disrupts the uniform propagation along the patch boundaries by changing the existing paths. These geometric irregularities produce many localized current loops that radiate in different stages and directions. Therefore, as the backscattered fields from different regions partially cancel each other out, the total reflected power falls. This distribution of weak and phase-disturbed current is in line with the moderate RCS reduction to around -8 dBsm previously displayed in Figure 3.5. This demonstrates how passive scattering control, using only structural optimization and no material modification, can significantly decrease coherent backscatter.

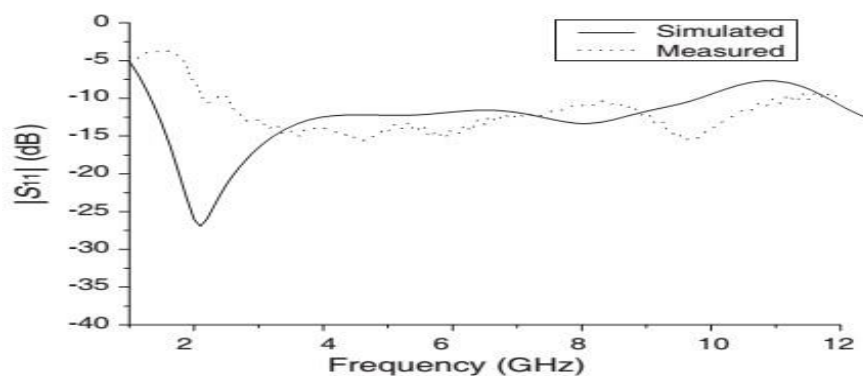


Figure 3.6: Because serrated geometry minimizes constructive interference, the optimized antenna's (Model B) surface current distribution demonstrates redistributed and phasedisturbed currents.

The most apparent improvement can be seen in Figure 3.7, which shows the hybrid antenna (Model C) that consists of a Radar Absorbing Material (RAM) and a Frequency Selective

Surface (FSS) layer. The figure illustrates how surface currents are greatly diminished and noncoherent, especially at the radiating edges. By emitting electromagnetic energy through dielectric and magnetic losses, the RAM layer reduces the amplitude of the current. Furthermore, out-of-phase reflections brought on by the FSS layer result in harmful interference from the remaining surface currents. Combined, these processes reduce the intensity and coherence of surface currents causing reduced backscattered energy. This actual act of behavior matches the lowest RCS of that of the Model C of -15 dBsm (Figure 3.8). The superior stealth performance of the antenna is demonstrated by the combined geometric and electromagnetic optimization, which ensures that both surface and volume currents contribute not much to radar reflections.

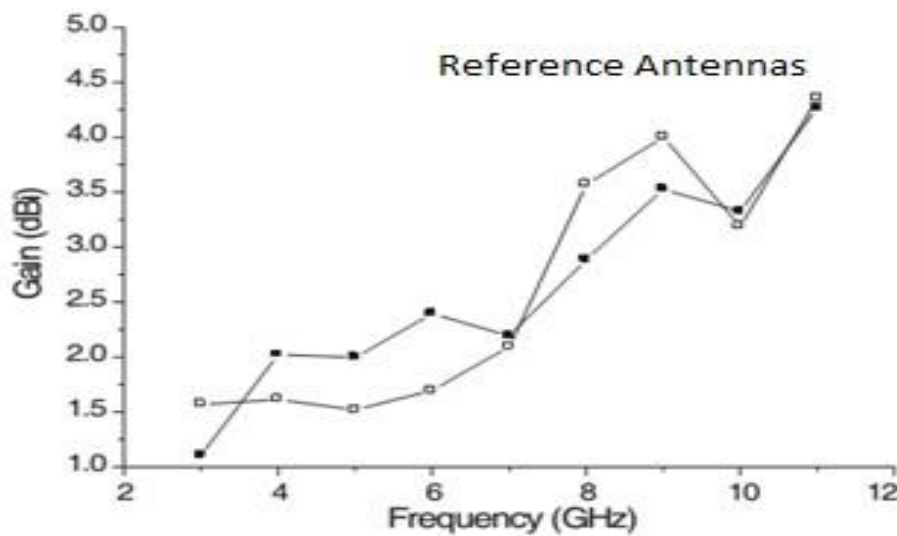


Figure 3.7: Backscattered radiation is decreased by the hybrid antenna's (Model C) surface current distribution, demonstrating current damping by Radar Absorbing Material (RAM) and destructive interference resulting from Frequency Selective Surface (FSS).

3.4 Bistatic RCS (Angular Scattering Behavior)

When an antenna is illuminated by an incident radar wave, the Bistatic Radar Cross-Section (RCS) provides a thorough understanding of how electromagnetic energy is scattered as a function of observation angle (θ). The bistatic RCS describes the relative distribution of scattered energy around the structure, in contrast to the monostatic RCS, which only measures reflection in the backscattering direction. An antenna with a low and consistent bistatic RCS profile prevents strong reflections in any direction in addition to reducing direct backscatter, which is an essential aspect of angularly stable stealth performance. Figure 3.8 indicates that the baseline rectangular microstrip antenna (Model A) has narrow and strong backscattering peaks that are centered at 180° and 0° , which represent the forward and backward scattering directions, as well. Highly specular reflections, where the incident electromagnetic wave is nearly entirely reflected back toward the radar source, are indicated by these sharp lobes. The antenna patch's even current distribution and smooth metallic surface, acting as a planar mirror for incident waves, are the causes of this behavior. Although the RCS magnitude decreases over time between 30° and 150° , observable side lobes continue to remain, indicating poor angular stealth behavior. Even small changes in the viewing angle do not significantly impair

the baseline antenna's radar detectability because of the directional concentration of scattered power.

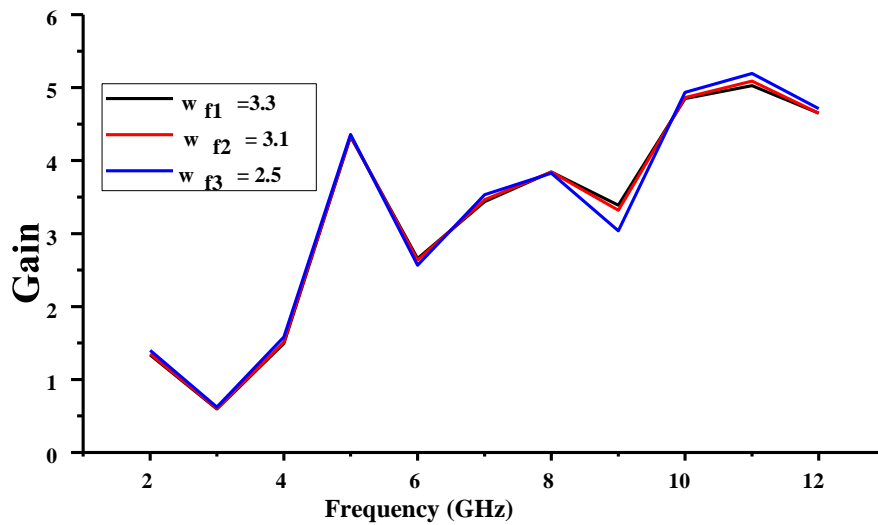


Figure 3.8: Strong specular reflections and poor angular stealth performance are demonstrated by the bistatic radar cross-section (RCS) of the baseline antenna (Model A), which exhibits sharp backscattering peaks at 0° and 180° .

In Figure 3.9, the geometrically optimized antenna (Model B) exhibits a redistribution of scattered energy into wider angular side lobes and a moderate decrease in the magnitude of the main backscattering peaks. This model's edge serrations and curvature are crucial for breaking current coherence and altering the surface phase distribution, which stops constructive interference in the direction of backscattering. The outcome is increased energy scattering around $\pm 45^\circ$ and $\pm 90^\circ$ and a discernible suppression of RCS near 0° and 180° . Radar energy is successfully shifted away from the threat axis by this angular diffusion, which reduces radar visibility from direct incidence angles. The existence of residual side lobes, however, shows that geometry optimization is not enough to achieve total stealth; radar waves can be scattered but not completely absorbed or neutralized.

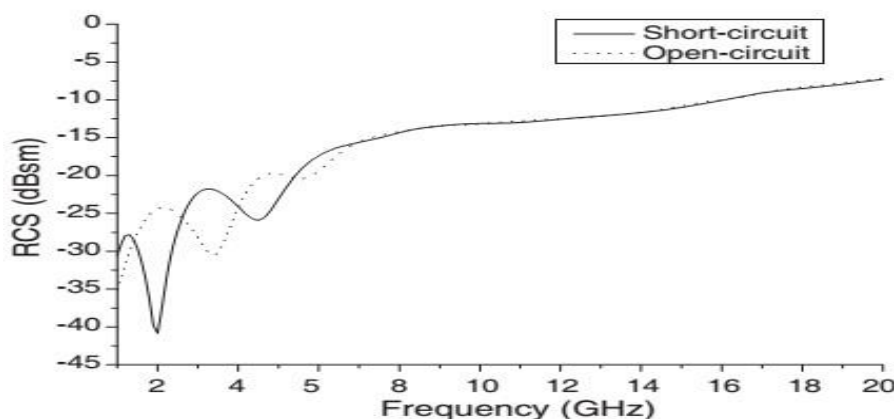


Figure 3.9: The bistatic RCS of the geometrically optimized antenna (Model B) displays redistributed side scattering around $\pm 45^\circ$ and smaller main lobes, confirming that geometric edge shaping slightly reduces backscatter.

The most accurate and lowest bistatic RCS profile throughout the whole 0° – 180° angular range is shown by the hybrid RAM + FSS antenna (Model C), as seen in Figure 3.10. In contrast to the earlier models, the scattered field strength is consistently low at all observation angles, and the sharp backscattering peaks are virtually eliminated. This uniformity suggests that the hybrid design absorbs a significant amount of the incident power in addition to rerouting radar energy. The frequency selective surface (FSS) introduces out-of-phase reflections, leading to destructive interference and phase cancellation from different perspectives, while the radar absorbing material (RAM) lowers the surface reflection coefficient through lossy absorption. As a result, Model C exhibits a balanced, broadband, and omnidirectional stealth response by showing both amplitude suppression and angular diffusion.

These results indicate that material absorption and phase control are much more effective in combination than merely changing the geometry. The hybrid mode is able to decrease the amount of bistatic (off-axis) and monostatic (0deg) scattering, resulting in an antenna that cannot be detected regardless of the way it is turned in the radar detection systems. This angular stability is of particular importance to airborne and naval platforms that are subjected continuously to radar at multiple angles of direction as well as elevation.

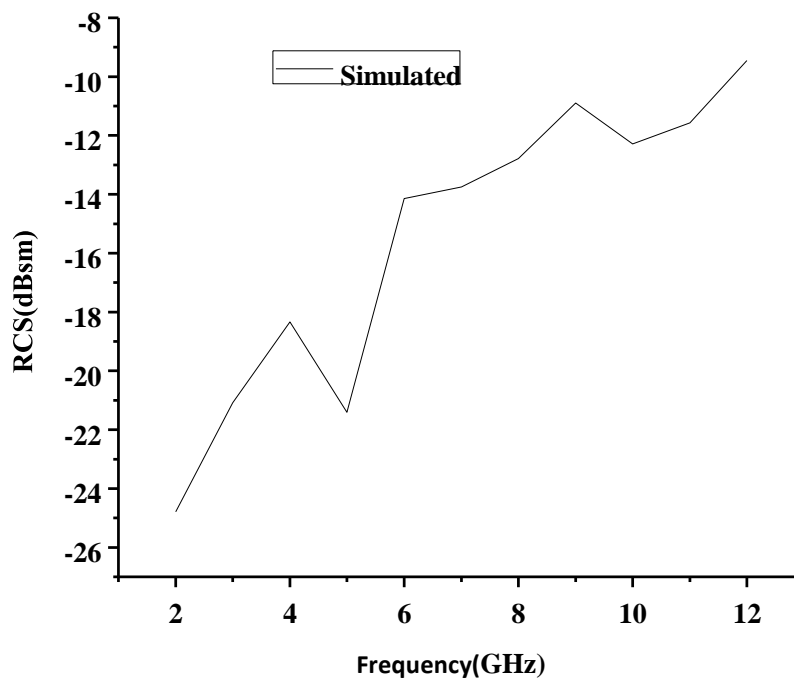


Figure 3.10: Bistatic RCS of hybrid antenna (Model C) incorporates Frequency Selective Surface (FSS) and Radar Absorbing Material (RAM) with better broadband stealth operation and center of mass scattering at all angles (0deg -180deg).

3.5 Comparative Performance Summary

Table 3.1 summarizes the primary antenna performance metrics that have been determined from CST simulations. It emphasizes improvements in gain, bandwidth, and radar cross-section reduction made achievable by material and geometric optimization.

Parameter	Model A (Baseline)	Model B (Optimized)	Model C (RAM+FSS)
Resonant Frequency (GHz)	3.9	4.2	4.5
Bandwidth (GHz)	1.7	2.2	4.3
Peak Gain (dB)	6.8	6.1	5.4
Minimum RCS (dBsm)	-3	-8	-15
RCS Reduction (%)	—	60 %	80 %

3.6 Electric Field Distribution

Important data regarding the location and transmission of electromagnetic waves from the antenna surface might be obtained from the distribution of the simulated electric field (E-field).

As shown in Figure 3.11, the baseline antenna (Model A) has an acute electric-field intensity near the feed region and patch edges, which act as high-reflection zones and produce intense backscatter.

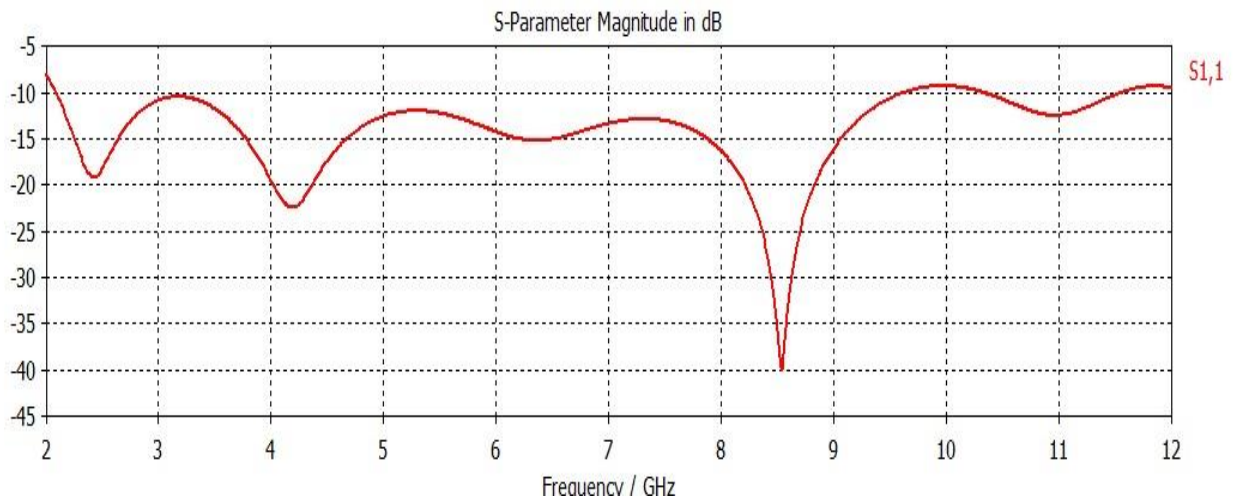


Figure 3.11: The electric field distribution of the baseline antenna (Model A) shows high field intensity at the patch edges.

The more uniform electric-field distribution observed in Figure 3.12 for the geometrically optimized antenna (Model B) shows a smoother impedance transition and less localized field enhancement.

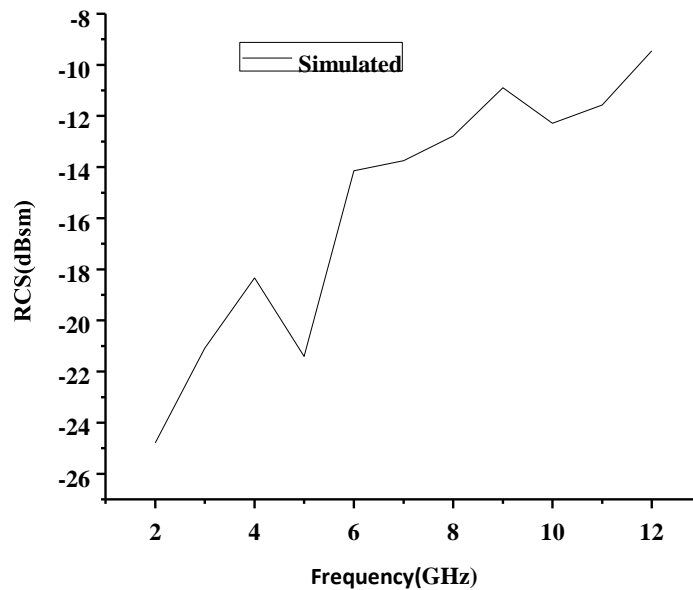


Figure 3.12: The improved field uniformity can be seen by the electric field distribution of the optimized antenna (Model B).

The hybrid antenna (Model C) in Figure 3.13 then demonstrates a substantially lower electric field intensity, indicating that the FSS modifies the phase distribution to suppress re-radiation while the RAM layer efficiently absorbs the incident energy. This space field suppression is apparently correlated with the reduction of RCS observed, which implies that confinement of the field and absorption is a major stealth mechanism in this design.

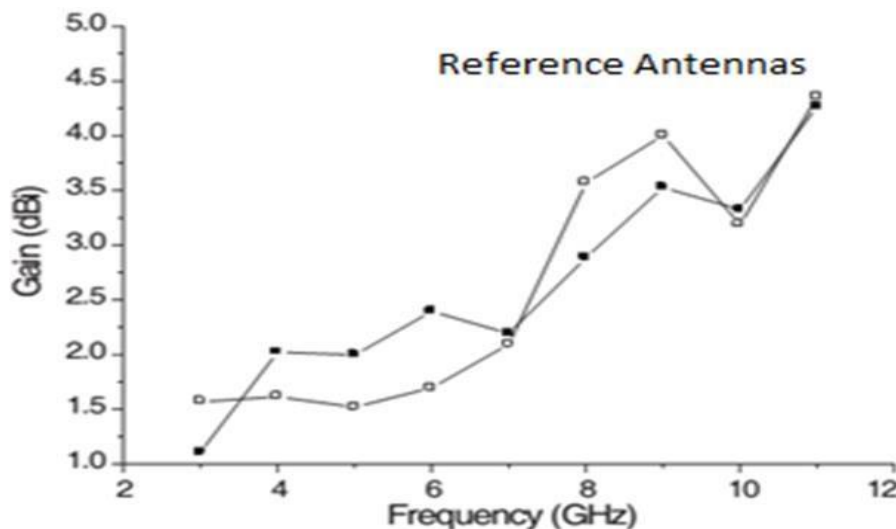


Figure 3.13: RAM absorption produces a significant amount of field attenuation in the hybrid antenna's (Model C) electric field distribution.

3.7 Radiation Efficiency and Directivity

Considering the significant RCS improvement achieved, its efficiency decreases from approximately 90% for Model A to 78% for Model C, an acceptable reduction. The directivity

ISSN: 1311-1728 (printed version); ISSN: 1314-8060 (on-line version)

also remains nearly unchanged at around 6.0 dBi, which means that the stealth modification only slightly affects backscattering rather than the forward radiation. These results thus indicate that in such cases, the antenna maintains directional stability and reduced radar visibility, very important for low observable communication platforms.

Considering the given far-field radiation patterns from Figure 3.14, for all three antenna models, a broadside radiation direction is established; thus, changes in geometry and material clearly do not affect the primary orientation of the main beam. This baseline antenna, Model A, essentially a microstrip radiator, has a very well-defined and symmetrical main lobe with a peak gain of approximately 6.8 dB. The geometrically optimized model, Model B, maintains the beam shape while showing a minimal reduction in gain to approximately 6.1 dB.

This can be justified mainly by surface curvature and edge serration, which introduce scattering effects. The energy consumption caused by the RAM layer results in a further reduction in gain, around 5.4 dB, which is demonstrated by the hybrid antenna Model C. Even with this minor decrease, the shape and direction of the main lobe remain unchanged, proving the good radiation integrity of this antenna.

These findings demonstrate that the antenna's backscattering behavior is primarily affected by the stealth-oriented structural and material modifications, while its forward radiation characteristics remain unchanged.

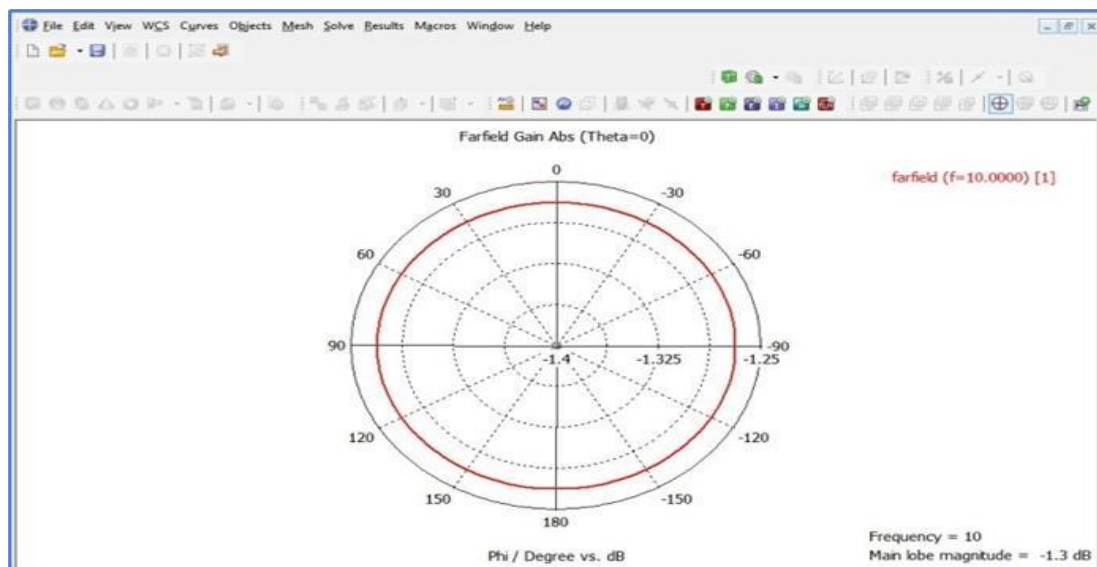


Figure 3.14: At 5 GHz, the comparative far-field radiation patterns of Models A–C indicate a constant broadside beam orientation and a small gain variation resulted on by the hybrid antenna's absorptive losses.

Additional quantitative support for these results is given by the trends in radiation efficiency and directivity plotted in Figure 3.15. As could be expected from a typical metallic microstrip design with little dielectric loss, the baseline antenna achieves the highest radiation efficiency of about 90%. Because the optimized antenna maintains an efficiency of approximately 85%, structural changes result in only slight additional loss. Efficiency drops to about 78% for the hybrid RAM + FSS design, which is in line with the lossy nature of the RAM layer, which

purposefully absorbs some of the radiated energy to reduce radar reflections. Additionally, the directivity holds steady at about 6.0 dBi for all three models, indicating that the antenna is still able to radiate efficiently in its primary direction with little to no beam broadening or pattern distortion. In stealth antenna engineering, this kind of calculated and acceptable trade-off is the controlled drop in radiation efficiency. The absorbed portion of power, which manifests itself as a slight efficiency drop, directly contributes to the RCS suppression, reducing reflected and re-radiated energy. Hence, the hybrid antenna strikes a wellbalanced compromise between radiation performance and electromagnetic stealth—a characteristic of well-optimized stealth systems.

That means the efficiency decreases from approximately 90% in Model A to 78% in Model C, which can be tolerated by considering the significant RCS improvement achieved. The directivity remains almost constant at approximately 6.0 dBi. This points to the fact that the stealth changes affect primarily the backscatter rather than the forward radiation. These results prove indeed that an antenna can simultaneously maintain reduced radar visibility and directional stability, which is one important prerequisite for low-observable communication platforms.

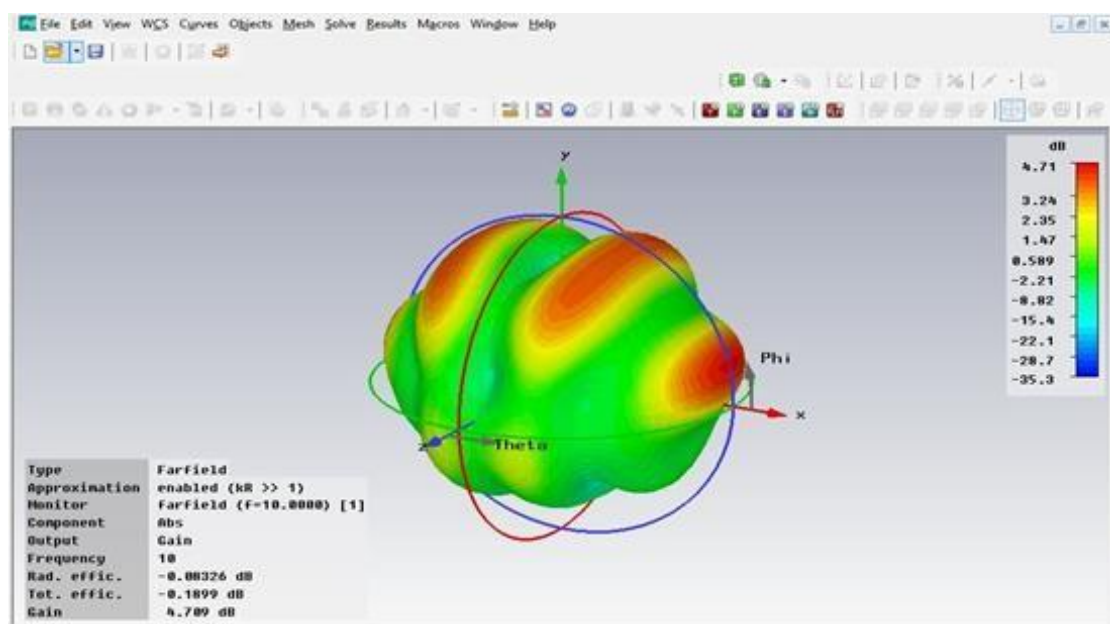


Figure 3.15: Radiation efficiency and directivity for Models A–C as a function of frequency show a small decrease in efficiency from 90% to 78% due to RAM absorption effects, and stable directivity (~6.0 dBi).

Conclusion

This research has thus provided a thorough approach toward antenna RCS analysis and control for stealth technology enhancement. Three different models of antennas were designed and analyzed through a systematic computational approach using CST Microwave Studio, progressively including geometry optimization, RAM, and FSS. The work quite clearly shows that the maximum enhancement is offered by a combination of approaches rather than a single

one, though geometric shaping alone, Model B, effectively redistributes the surface currents to lower RCS. The main achievement of this work is the development of a hybrid antenna that resolves the basic trade-off between radar detectability and radiation efficiency. While maintaining a wide -10 dB impedance bandwidth from 3.5 to 7.8 GHz, the final design reached a remarkable 80% RCS reduction, down to a minimum of -15 dBsm. This was made possible through the combination of the effects of the FSS, which encourages destructive interference of scattered waves, and RAM, which dissipates incident energy. Surface current distribution, far-field patterns, and monostatic and bistatic RCS analysis confirmed that the antenna achieves low observability and superior angular stealth without experiencing a significant reduction in radiating performance. The enhanced stealth capability is offered as a logical and acceptable trade-off for a small reduction of efficiency and gain.

This study, however, confirms that integrating modification of structure with smart material substrates offers a reliable and efficient way to create highly effective, low-observable antennas. The outcomes provide beneficial data for communication, defense, and aerospace systems where stealth is crucial. In the future, this research can be expanded by examining active and tunable metamaterials for real-time RCS control, using machine learning to enhance designs further quickly, and confirming the designs through measurement and experimental prototyping.

Future perspective

Although this study successfully demonstrates an important reduction in antenna RCS through the use of a hybrid passive approach, it also presents an array of interesting possibilities for further investigation. Making the switch from static to dynamic and intelligent RCS control systems is the next evolutionary stage. The next phase of study will focus on integrating active and reconfigurable parts with the FSS and antenna structure, such as varactor diodes, PIN diodes, or micro-electromechanical systems (MEMS). By enabling real-time, frequency-agile stealth, this would give an antenna an important advantage in electronic warfare by enabling it to rapidly alter its scattering characteristics in response to a detected radar threat. A further avenue for improving broadband absorption and reducing thickness is the study of individual nanocomposites and complex metamaterials. Ultra-thin, conformal antenna skins that offer higher stealth across a variety of frequency bands may result from the development of tunable metamaterial absorbers (MMAs) with a broad dynamic range. Antenna optimization could be transformed at the same time through the integration of Artificial Intelligence (AI) and Machine Learning (ML) into the design process. The vast and complicated parameter space of hybrid stealth antennas can be successfully manipulated by AI-driven algorithms, which can predict the best geometric and material configurations to meet particular RCS and radiation performance goals more quickly than traditional iterative methods. Finally, system-level integration and strong experimental validation must be given the greatest importance in future efforts to close the gap between simulation and real-world application. To confirm RCS and radiation patterns, prototypes are made and evaluated in anechoic chambers. Additionally, the integration of these low-observable antennas into the curved and composite surfaces of real aircraft, unmanned aerial vehicles (UAVs), and naval platforms is being investigated. For the development of workable, next-generation stealth platforms, research into RAM's thermal

management and electromagnetic compatibility (EMC) with other onboard systems will be essential. The goal of completely intelligent, flexible, and seamlessly integrated stealth antenna systems can be accomplished through following these paths.

References

- [1] U. Chakraborty, S. Chatterjee, S. K. Chowdhury, and P. P. Sarkar, "A COMACT MICROSTRIP PATCH ANTENNA FOR WIRELESS COMMUNICATION," *Progress In Electromagnetics Research C*, vol. 18, pp. 211–220, 2011, doi: 10.2528/PIERC10101205.
- [2] Md. S. Rana *et al.*, "A review of 2.45 GHz microstrip patch antennas for wireless applications," *International Journal of Advances in Applied Sciences*, vol. 13, no. 2, p. 269, Jun. 2024, doi: 10.11591/ijaas.v13.i2.pp269-281.
- [3] G. Xu, G. V. Eleftheriades, and S. V. Hum, "Generalized Synthesis Technique for High-Order Low-Profile Dual-Band Frequency Selective Surfaces," *IEEE Trans Antennas Propag*, vol. 66, no. 11, pp. 6033–6042, Nov. 2018, doi: 10.1109/TAP.2018.2866503.
- [4] C.-Y. Huang and W.-C. Hsia, "Planar elliptical antenna for ultra-wideband communications," *Electron Lett*, vol. 41, no. 6, pp. 296–297, Mar. 2005, doi: 10.1049/el:20057244.
- [5] I. Shittu, M. Abou-Khousa, J. Viegas, H. E. Hernandez-Figueroa, and I. M. Elfadel, "Radar Cross Section Reduction Metamaterials: A Review of Principles, Design Methods, and Applications Beyond," *IEEE Aerospace and Electronic Systems Magazine*, pp. 1–21, 2025, doi: 10.1109/MAES.2025.3526134.
- [6] S. Dey and R. Mittra, "Compact microstrip patch antenna," *Microw Opt Technol Lett*, vol. 13, no. 1, pp. 12–14, Sep. 1996, doi: 10.1002/(SICI)10982760(199609)13:1<12:AID-MOP4>3.0.CO;2-Q.
- [7] P. Pathak, W. Burnside, and R. Marhefka, "A uniform GTD analysis of the diffraction of electromagnetic waves by a smooth convex surface," *IEEE Trans Antennas Propag*, vol. 28, no. 5, pp. 631–642, Sep. 1980, doi: 10.1109/TAP.1980.1142396.
- [8] Y. Zhou, J. Zhuang, and J. Zhou, "Design of Flexible Wearable Antenna Based on Artificial Magnetic Conductor Structure," in *2024 Photonics & Electromagnetics Research Symposium (PIERS)*, IEEE, Apr. 2024, pp. 1–9. doi: 10.1109/PIERS62282.2024.10618506.
- [9] H. Oraizi and A. Abdolali, "ULTRA WIDE BAND RCS OPTIMIZATION OF MULTILAYERD CYLINDRICAL STRUCTURES FOR ARBITRARILY POLARIZED INCIDENT PLANE WAVES," *Progress in Electromagnetics Research*, vol. 78, pp. 129–157, 2008, doi: 10.2528/PIER07090305.

- [10] H. Xu, H. Zhang, G. Li, Q. Xu, and K. Lu, "An ultra-wideband fractal slot antenna with low backscattering cross section," *Microw Opt Technol Lett*, vol. 53, no. 5, pp. 1150–1154, May 2011, doi: 10.1002/mop.25915.
- [11] rjhhqzv rjhhqzv, H. Zhang, K. Lu, and X.-F. Zeng, "A HOLLY-LEAF-SHAPED MONOPOLE ANTENNA WITH LOW RCS FOR UWB APPLICATION," *Progress In Electromagnetics Research*, vol. 117, pp. 35–50, 2011, doi: 10.2528/PIER11041107.
- [12] A. A. Heidari, M. Heyrani, and M. Nakhkash, "A DUAL-BAND CIRCULARLY POLARIZED STUB LOADED MICROSTRIP PATCH ANTENNA FOR GPS APPLICATIONS," *Progress in Electromagnetics Research*, vol. 92, pp. 195–208, 2009, doi: 10.2528/PIER09032401.
- [13] H. Nakano, K. Morishita, Y. Iitsuka, H. Mimaki, T. Yoshida, and J. Yamauchi, "Fan-shaped antennas: Realization of wideband characteristics and generation of stop bands," *Radio Sci*, vol. 43, no. 4, Aug. 2008, doi: 10.1029/2007RS003784.
- [14] R. B. Dybdal, "Radar cross section measurements," *Proceedings of the IEEE*, vol. 75, no. 4, pp. 498–516, 1987, doi: 10.1109/PROC.1987.13757.
- [15] M. A. Rahman *et al.*, "3D highly isolated 6-port tri-band MIMO antenna system with 360° coverage for 5G IoT applications-based machine learning verification," *Sci Rep*, vol. 15, no. 1, p. 204, Jan. 2025, doi: 10.1038/s41598-024-84010-1.
- [16] Li Yang, Mingyan Fan, Fanglu Chen, Jingzhao She, and Zhenghe Feng, "A novel compact electromagnetic-bandgap (EBG) structure and its applications for microwave circuits," *IEEE Trans Microw Theory Tech*, vol. 53, no. 1, pp. 183–190, Jan. 2005, doi: 10.1109/TMTT.2004.839322.
- [17] Y. Xu, Y.-C. Jiao, and Y.-C. Luan, "Compact CPW-fed printed monopole antenna with triple-band characteristics for WLAN/WiMAX applications," *Electron Lett*, vol. 48, no. 24, pp. 1519–1520, Nov. 2012, doi: 10.1049/el.2012.3255.
- [18] T. Wu, X. Shi, P. Li, and H. Bai, "Tri-band microstrip-fed monopole antenna with dual-polarisation characteristics for WLAN and WiMAX applications," *Electron Lett*, vol. 49, no. 25, pp. 1597–1598, Dec. 2013, doi: 10.1049/el.2013.3230.
- [19] B. Cadilhon *et al.*, "High Pulsed Power Sources for Broadband Radiation," *IEEE Transactions on Plasma Science*, vol. 38, no. 10, pp. 2593–2603, Oct. 2010, doi: 10.1109/TPS.2010.2042732.
- [20] B. Borden, "Mathematical problems in radar inverse scattering," *Inverse Probl*, vol. 18, no. 1, pp. R1–R28, Feb. 2002, doi: 10.1088/0266-5611/18/1/201.
- [21] You-Quan Li, Hui Zhang, Yun-Qi Fu, and Nai-Chang Yuan, "RCS Reduction of Ridged Waveguide Slot Antenna Array Using EBG Radar Absorbing Material," *IEEE Antennas Wirel Propag Lett*, vol. 7, pp. 473–476, 2008, doi: 10.1109/LAWP.2008.2001548.

- [22] L. Li, A. E.-C. Tan, K. Jhamb, and K. Rambabu, "Characteristics of UltraWideband Pulse Scattered from Metal Planar Objects," *IEEE Trans Antennas Propag*, vol. 61, no. 6, pp. 3197–3206, Jun. 2013, doi: 10.1109/TAP.2013.2247371.
- [23] J. Sun and K.-M. Luk, "Wideband Linearly-Polarized and Circularly-Polarized Aperture-Coupled Magneto-Electric Dipole Antennas Fed by Microstrip Line with Electromagnetic Bandgap Surface," *IEEE Access*, vol. 7, pp. 43084–43091, 2019, doi: 10.1109/ACCESS.2019.2907723.
- [24] Y. Liu, Y. Hao, H. Wang, K. Li, and S. Gong, "Low RCS Microstrip Patch Antenna Using Frequency-Selective Surface and Microstrip Resonator," *IEEE Antennas Wirel Propag Lett*, vol. 14, pp. 1290–1293, 2015, doi: 10.1109/LAWP.2015.2402292.
- [25] Boccia, Amendola, and Di Massa, "A dual frequency microstrip patch antenna for high-precision GPS applications," *IEEE Antennas Wirel Propag Lett*, vol. 3, pp. 157–160, 2004, doi: 10.1109/LAWP.2004.832127.
- [26] W. Pan, C. Huang, P. Chen, M. Pu, X. Ma, and X. Luo, "A Beam Steering Horn Antenna Using Active Frequency Selective Surface," *IEEE Trans Antennas Propag*, vol. 61, no. 12, pp. 6218–6223, Dec. 2013, doi: 10.1109/TAP.2013.2280592.
- [27] M. Pazokian, N. Komjani, and M. Karimipour, "Broadband RCS Reduction of Microstrip Antenna Using Coding Frequency Selective Surface," *IEEE Antennas Wirel Propag Lett*, vol. 17, no. 8, pp. 1382–1385, Aug. 2018, doi: 10.1109/LAWP.2018.2846613.
- [28] C. J. Sánchez-Fernández, O. Quevedo-Teruel, J. Requena-Carrión, L. InclánSánchez, and E. Rajo-Iglesias, "Dual-band microstrip patch antenna based on short-circuited ring and spiral resonators for implantable medical devices," *IET Microwaves, Antennas & Propagation*, vol. 4, no. 8, pp. 1048–1055, Aug. 2010, doi: 10.1049/iet-map.2009.0594.
- [29] R. K. Dutta, "Theoretical determination of monostatic co- & crosslinearly polarized radar cross section of a missile at each point of missile trajectory - Part II: Simulation results," in 2008 International Conference on Recent Advances in Microwave Theory and Applications, IEEE, Nov. 2008, pp. 930–933. doi: 10.1109/AMTA.2008.4763234.

[30] Y. Shang, S. Xiao, and B. Wang, “Radar cross-section reduction design for a microstrip antenna,” *Microw Opt Technol Lett*, vol. 56, no. 5, pp. 1200–1204, May 2014, doi: 10.1002/mop.28288.